Tutorial

Enhanced-Backscattering and Enhanced-Backreflection Fibers for Distributed Optical Fiber Sensors

T. Lee, M. Beresna, A. Masoudi and G. Brambilla, *Member, IEEE*

***Abstract*—Most distributed optical fiber sensors rely on commercially available telecom fibers, which are low-loss, inexpensive, and standardized. In the last few years, significant effort has been made to develop optical fibers optimized for specific sensing applications, with the view of improving the signal-to-noise ratio (SNR) or extending the distance over which distributed optical fiber sensors (DOFS) operate. This tutorial reviews the efforts made by the scientific community towards the development of enhanced backscattering fibers and enhanced backreflection fibers, with a focus on DOFS.**

***Index Terms*—Optical fibers; Optical fiber sensors; Fiber gratings; Optical reflection; Sensor arrays; Sensor systems**

I. Introduction

Since their first use in bundles for endoscopy by Heinrich Lamm in 1930, optical fibers have found a myriad of applications in optical fiber sensors, ranging from chemical to physical, biological, and nuclear. Optical fiber sensors are typically categorized as intrinsic or extrinsic. In intrinsic sensors, the optical fiber is used as a transducer to convert the measurand into an optical signal that can be measured at the detector. In extrinsic sensors, the light signal is modulated by the external perturbation in a location different from the optical fiber, which then merely acts as data transmission channel between the sensing and detecting systems. Of the two classes of sensors, optical fibers gained extreme importance for intrinsic sensors, as their properties can be tailored to the targeted measurand.

Intrinsic sensors can be further classified as point, quasi-distributed, and distributed sensors, according to whether the measurement occurs in a single location, in a discrete/relatively small number of locations, or continuously along the optical fiber length, respectively. The fiber optic gyroscope [1] is probably the most successful point sensor and has found various applications in aerospace and, more recently, in submarines. Fiber Bragg Gratings (FBGs), with their ability to multiplex, operate remotely and be unaffected by electromagnetic interference, have attracted significant interest in temperature, strain and in structural health monitoring, becoming the most successful quasi-distributed sensor [2]. Finally, distributed optical fiber sensors (DOFSs), with their capability to measure strain and/or temperature distributions along the whole length of fiber (often beyond 40 km), represent the most successful optical fiber sensors, as they effectively allow for the simultaneous monitoring of thousands of points at an unrivaled low cost [3].

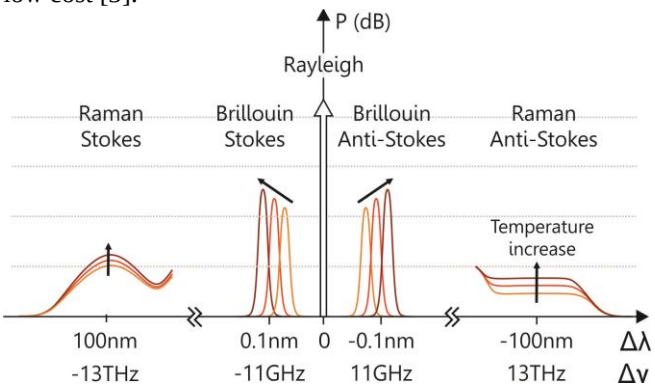

Fig. 1. Schematic diagram comparing scattering processes in silica optical fibers and their spectrum with respect to the frequency of the incident light. Arrows indicate spectral change trend with increasing temperature.

DOFSs monitor physical measurands by interrogating the sensing fiber with a frequency scanned or pulsed light source and then analyzing the resulting backscattered light which can arise from Raman [4], Brillouin [5], or Rayleigh [6] effects (Fig. 1). Raman scattering relies on inelastic scattering between the incident photon and molecular vibrations in the glass network, known as optical phonons. As the Stokes and anti-Stokes intensities in silicate optical fibers are dependent on temperature only, their comparison allows for DOFSs [7-9] that can measure temperatures with resolutions often better than 1 °C over distances exceeding 10 km. Brillouin scattering is generated by inelastic scattering between the incident photon and acoustic phonons; it is dependent on both temperature and strain, thus allowing simultaneous determination of both [10-12], although with significant cross-sensitivity issues. Brillouin-based DOFSs are particularly useful for the continuous monitoring of absolute strain along the fiber. Rayleigh scattering is the only elastic scattering mechanism used for distributed sensing and it relies on microscopic spatial fluctuations in the glass density in the core of the optical fiber. When the incident light interacts with these density fluctuations, also known as inhomogeneities, it forms an oscillating dipole at each inhomogeneity that radiates an

electromagnetic field with the same frequency and polarization as the incident light. The re-radiated light is commonly known as Rayleigh scattering.

Rayleigh scattering provides a significantly larger signal level compared with inelastic scattering mechanisms [13,14]; in silica optical fibers it is ~16 dB higher than the Brillouin signal, and ~30 dB higher than Raman (Fig. 1). Rayleigh scattering has found numerous applications, including the measurement of shape [15], strain, temperature and pressure [16], magnetic field [17], and dosimetry [18]. Yet, the most successful DOFSs exploiting Rayleigh scattering are related to the measurement of relative strain changes in time, e.g. vibrations [19-20]. Distributed acoustic sensing (DAS), also called distributed vibration sensing (DVS), relies on Rayleigh scattering to monitor vibrations over lengths exceeding 40 km from a single end. The use of long linearly frequency-modulated pulses and specialty fibers has allowed reaching lengths in excess of 170 km [21]. Moreover, Rayleigh-based DOFSs have investigated the possibility to use multicore [22] or multimode [23-25] fibers. The latter increases the threshold power for nonlinear effects, thus allowing a higher probe pulse energy to be used for a greater SNR. Furthermore, a larger fraction of the Rayleigh backscatter can be captured, and signal fading is reduced by detecting several fiber modes in parallel. Rayleigh scattering has also been used over short lengths of optical fibers for medical applications [26], where mm spatial resolutions (typically less than a meter) are required.

As the intensity of a signal that is propagating along the optical fiber exponentially decreases due to the natural optical fiber attenuation, there is a distance beyond which the reduction in the intensity of the backscattered signal level makes measurements inaccurate and unreliable. Background environmental noises can yield an even poorer SNR as the increased noise level further restricts DOFS sensitivity and operating range.

While in the past DOFSs implemented various techniques such as signal averaging or wavelet analysis to minimize the noise N at the denominator of SNR, in the last decade, research has focused on the development of novel optical fibers that could significantly enhance the signal S, especially by introducing low-loss backreflections. The next sections will compare backscattering and backreflection techniques, and review the various fibers investigated to maximize the SNR without compromising the loss.

II. BACKSCATTERING VS BACKREFLECTION

In glass optical fibers, attenuation is given by extrinsic factors (such as contamination with metal/transition elements, hydroxyls, or particles) and by intrinsic factors (electronic bond absorption, vibrational absorption, and scattering). Telecom fibers have minimized the attenuation due to extrinsic factors and absorption to a level such that more than 80% of the total attenuation around 1550 nm is given by Rayleigh scattering [27]. In the last two decades, ultra-low-loss fibers have resulted from a reduced Rayleigh scattering achieved either by reducing the glass fictive temperature T_f in solid fibers [28] or by propagating most of the mode in air in hollow-core fibers [29]. T_f is defined as the temperature where glass and liquid have the same degree of disorder [30] and it is thus determined by the temperature dependence of viscosity, the glass thermal history [31] and its chemical composition [32, 33]. T_f ultimately determines the local fluctuations in the density and refractive index that are responsible for scattering.

When the fluctuations have a size larger than $\lambda/10$, scattering is described through the Lorenz–Mie–Debye solution of Maxwell equations and is called Mie scattering, which does not exhibit a strong wavelength dependence. In practice, optical fibers have fluctuations that are significantly smaller than 100 nm, thus scattering can be described through Rayleigh scattering, which has a wavelength dependence of λ^{-4}.

Standard telecom fibers such as G.652 have a scattering coefficient of ~0.0002 dB/m [3] which translates to a Rayleigh backscattered signal of -71 dB/m when multiplied by the capture fraction of the fiber. Hence, a 10 ns probe pulse with a peak power of 250 mW yields 7.6 nW of Rayleigh signal from the far-end of the sensing fiber which is relatively weak. Two approaches can be taken to increase the signal: increasing Rayleigh backscattering or introducing some type of reflectors, e.g. FBGs. Fig. 2 gives a schematic comparison between two fibers with the same attenuation, where the largest components are scattering (Fig. 2(a)) and backreflection (Fig. 2(b)).

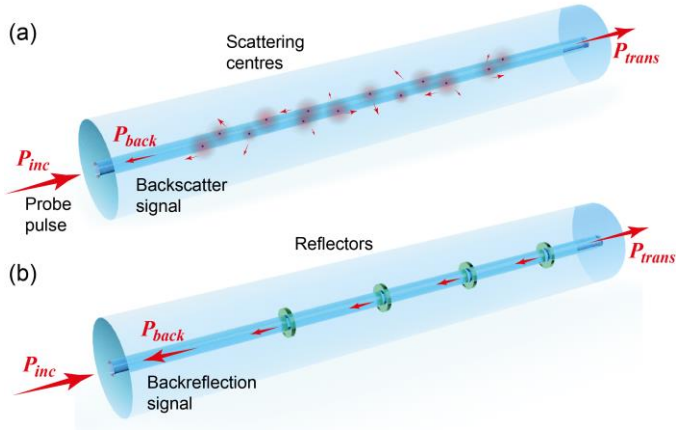

Fig. 2. Schematic comparison between (a) backscattering and (b) backreflection. In scattering media, incident light is scattered in many directions and only partially collected by the optical fiber and delivered to its input facet. In backreflection, most of the incident power reflected by the reflectors is directionally coupled into the mode propagating in the opposite direction, with negligible radiative losses in directions orthogonal to mode propagation.

It is important to point out that scattering occurs in all directions, and the fraction of light collected by the fiber core is limited by the numerical aperture (NA) of the optical fiber itself. In other words, some of the incident light will be scattered at angles that radiate out of the optical fiber, resulting in attenuation in the transmitted intensity.

In contrast to scattering, reflection provides directionality to the light components that are removed from the forward propagating mode. Reflection usually occurs at interfaces with different refractive indices and the fraction of power reflected is given by the Fresnel coefficient, which for normal incidence is proportional to the square of the ratio between the difference and the sum of the refractive indices of the two media on either

side of the interface. As shown in the schematic of Fig. 2(b), the overall backreflected power is larger than the backscattered power when the optical fiber attenuation is the same. While scattering can occur naturally in the glass, backreflection in optical fibers has to be engineered through induced refractive index changes.

The efficiency of modified fibers could be compared through the magnitude of the backscattering coefficient enhancement η_{enh} in relation to the standard telecom optical fiber:

$$\eta_{enh} = \frac{\beta_M}{\beta_{SMF28}} \quad (1)$$

where β_M and β_{SMF28} are the backscattering coefficients of modified and SMF-28 fibers, respectively.

However, this comparison does not take into account the possible increase in attenuation that is associated with an increase in Rayleigh scattering, which is a critical factor for long distance applications. Although a larger η_{enh} means a larger scattering at a given point within the fiber, a larger attenuation means that the power incident on the section of the fiber of interest decreases with distance and the Rayleigh signal is further attenuated on its way to the detector. Therefore, the distance over which the DOFS system can operate does not change significantly, and indeed is often worse (Fig. 3). while larger scattering coefficients are beneficial over shorter ranges, they are detrimental for long distance operation.

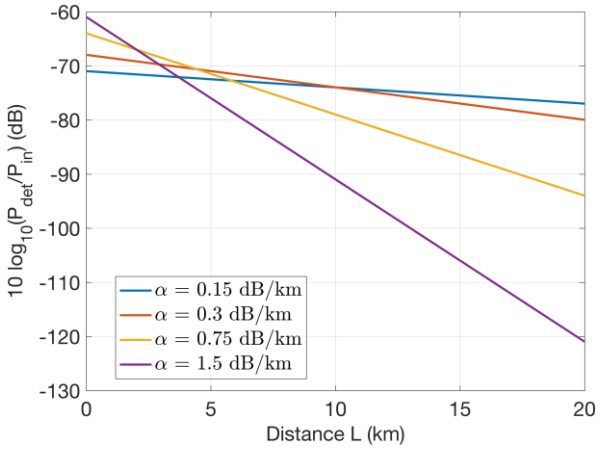

Fig. 3. Comparison of backreflected signal received by the detector for a 10ns pulse propagating in fibers with different values of scattering/attenuation coefficients. Each curve on the graph shows the normalized output power 10 $\log_{10}(P_{det}/P_{inc})$ for a fixed attenuation coefficient α, as a function of distance L [3]. Attenuation is assumed to be entirely due to scattering. The initial gain produced by stronger scattering is followed by a rapid decline in signal strength resulting in reduced operational range.

The round-trip attenuation of light in an optical fiber, α, in units of dB/km, is defined as:

$$\alpha = -\frac{10}{2L} \cdot C_{s-c} \cdot log_{10} \frac{P_{det}}{P_{inc}} \quad (2)$$

where L is the distance in km traveled by light into the optical fiber, P_{inc} is the power entering the optical fiber, P_{det} is the power collected at the front-end of the fiber, and $C_{S\text{-}C}$ is a coefficient that includes the Rayleigh scattering efficiency and the fiber collection efficiency [3].

While attenuation affects the signal exponentially with the distance through the Beer-Lambert law, Rayleigh scattering enhancement is independent of the distance. The performance of optical fibers in terms of the detected signal power can be better quantified by a quality factor Q_{enh}, which includes both attenuation and scattering and is normalized with respect to the performance of a conventional terrestrial telecom fiber SMF28. In decibel units, Q_{enh} can be expressed as:

$$Q_{enh} = 10 \cdot log_{10} \left[\frac{\beta_M \cdot 10^{-2L \cdot \frac{\alpha_M}{10}}}{\beta_{SMF28} \cdot 10^{-2L \cdot \frac{\alpha_{SMF28}}{10}}} \right]$$

$$= 10 \cdot log_{10} \left(\frac{\beta_M}{\beta_{SMF28}} \right) - 2L(\alpha_M - \alpha_{SMF28}) \quad (3)$$

$$= 10 \cdot log_{10}(\eta_{enh}) - 2L(\alpha_M - \alpha_{SMF28})$$

In Eq. (3), by setting Q_{enh} to 0 dB, it is possible to determine the length of fiber L_{enh} (in km) at which the gain provided by the Rayleigh scattering enhancement is compensated by the increased attenuation:

$$L_{enh} = \frac{10 \cdot log_{10}(\eta_{enh})}{2(\alpha_M - \alpha_{SMF28})} \quad (4)$$

L_{enh} is possibly the most interesting parameter for DOFS applications, as it provides the distance over which the sensing system can extend its operation assuming the remaining parameters of the DOFS are kept constant.

III. ENHANCED BACKSCATTERING FIBERS

A. *Post-fabrication treatments*

The first attempts to increase the backscattered signal in fibers were performed by increasing the level of Rayleigh scattering in telecom optical fibers. This was achieved by processing optical fibers after they had been fabricated [34, 35]. Post-fabrication treatments have been performed on two types of fibers commonly used in sensing: terrestrial telecom fibers, as they provide the minimum attenuation, and photosensitive optical fibers, which allow for an easy inscription of FBGs.

At the end of the last century, it was noticed that glass exposed to UV radiation exhibits an increase in Rayleigh scattering [34]. In 2015, a fiber was illuminated with 213 nm wavelength from the 5th harmonic of a 1064 nm solid-state laser. The 200 μm spot size was translated over the fiber at a speed of 50 μm/s, providing a uniform exposure time of 4 s [35]. This technique provided a backscattering increase of $\eta_{enh(dB)}$~20 dB, attributed to an increase in color centers in the fiber, which enhance the overall Rayleigh scattering. However, loss also increased by a similar value, thus providing an overall negative Q_{enh} of -10 dB, i.e. a worse performance to that of SMF28 telecom fiber in long distance applications. This effect was however still deemed useful for short distance applications,

where the enhanced scattering reduced the dynamic range requirements on the detection system and increased the tolerable environmental noise level. The scattering enhancement has been explained by the creation of defects and further experiments aimed at optimizing scattering yielded a 20 to 25 fold improvement, thus an overall maximum $\eta_{enh(dB)}$ of 14 dB [36].

As femtosecond lasers allow modification of the glass refractive index without prior removal of the polymer coating and do not require additional dopants or processes to increase the material photosensitivity, their potential for fiber processing seemed even more promising. A laser system operating at a 250 kHz repetition rate was used to deliver linearly polarized 300 fs pulses at 800 nm with energy up to 200 nJ to a cylindrical telescope that was used to focus the beam into a terrestrial telecom optical fiber. The fiber was translated under the beam using a reel-to-reel setup and Rayleigh backscattering was measured in real-time using a backscattering reflectometer (OBR Luna 4600). The observed enhancement was 40-45 times [37], or $\eta_{enh(dB)}$ ~ 16.5 dB. In this case, the enhanced Rayleigh backreflection was explained by the formation of nanogratings, which self-form under repeated pulse exposure and can provide extremely large refractive index changes (Δn~10^{-2}), often accompanied by strong scattering.

Quasi-distributed backscattering signal enhancement is another path actively explored by several research groups. The combination of hydrogen-loading and UV exposure has been widely used in the past in the manufacturing of FBGs in telecom optical fibers. In 2019, this technique was investigated to enhance optical fiber Rayleigh scattering. An FBG was written at 25 μm/s using the fourth harmonic (λ = 266 nm) of a Q-switched Nd:YAG laser with 100 mW of power. While the grating's Bragg wavelength was outside the region of interest, thus light propagating in the fiber did not experience any direct Bragg reflection from the grating, the Rayleigh scattering nonetheless increased due to material structural changes. This technique showed a radical increase in the backscattered signal of about ~6300 times [38] ($\eta_{enh(dB)}$=38 dB). Yet, hydrogen loading is well known to be associated with an increase in loss that can exceed α~100 dB/km, which would outweigh the improvement in η_{enh} to produce a negative Q_{enh} of -164 dB and an additional length shorter than 1 km.

Post-fabrication treatments are time-consuming, as the processing speed is typically in the order of mm/s and thus impractically slow for scaling up to the tens of kilometers of fibers needed for longer range DOFS. In addition, Hydrogen loading often requires more than a week.

B. Compositional changes

An alternative approach to the post-fabrication treatment of telecom optical fibers is represented by the manufacture of novel optical fibers with different dopants, specifically designed to increase scattering.

Germanium concentration has been shown to affect Rayleigh scattering, with higher concentrations being more favorable for this purpose [39]. Experiments with a heavily-doped germanosilicate optical fiber (SM1500 from Fibercore) showed a 4.1 times larger Rayleigh backscattered signal ($\eta_{enh(dB)}$ ~ 6.1 dB) [40]. As this fiber also exhibits an attenuation of α=2 dB/km [41], ten times larger than that of a terrestrial telecom fiber α_{SMF}, the overall negative quality factor (Q_{enh}= -3 dB), makes it unsuitable for long-distance applications.

As larger germanium concentrations result in higher NA, smaller core size, and higher splice loss with telecom optical fibers, a double-clad fiber was envisaged [42]. Yet, the enhancement in Rayleigh scattering was a mere η_{enh}~1.3 dB, while the attenuation increased to α~ 0.4 dB/km, leading to Q_{enh}~ 0.9 dB.

Additional dopants such as Boron or Fluorine are claimed to boost the optical fiber core material inhomogeneity [43, 44], increase the refractive index fluctuations, and augment Rayleigh scattering. Yet, the moderate increment observed with other dopants has not provided sufficient momentum to expand research over different doping elements.

Optical fiber doping with nanoparticles has been deemed more promising, as their phase separation during optical fiber drawing or post-fabrication has been widely studied in the attempt to extend the amplification bandwidth of rare earth ions in silica fibers. The effect of nanoparticles on attenuation and Rayleigh scattering has been analyzed [45]. Nanoparticles can exhibit a large refractive index contrast with respect to the surrounding host medium, thus providing a larger Rayleigh scattering coefficient.

Zirconia-coated gold nanoparticles were doped into the core of an optical fiber preform and the drawn optical fiber was used for distributed temperature sensing up to 800°C by Optical Frequency Domain Reflectometry (OFDR) [46]. The fiber produced an enhancement both in backscattering and in attenuation but showed the possibility to perform temperature measurements with 1 cm spatial resolution over a 0.7 m length of fiber up to 800 °C.

Doping of a silica optical fiber with zirconia nanoparticles was also demonstrated [47]: the fiber was manufactured by the Modified Chemical Vapor Deposition (MCVD) method coupled with solution doping and exhibited a Rayleigh scattering improvement of $\eta_{enh(dB)}$ = 40 dB and losses of 2.8 dB/m. This provides a significantly negative Q_{enh}= -5540 dB. An 8 h annealing step at 800 °C induced an increased attenuation of 3.1 dB/m and increased the OFDR signal amplitude by 0.4 dB.

Gold nanoparticles have also been proposed as a dopant because of their extremely large scattering coefficient; for 1550 nm incident light, the best size of gold NPs for light enhancement was found to be 224 nm [48]. The spectral characteristics of optical fibers doped with gold nanoparticles under axial strain have been investigated [49].

An increased interest in Optical Backscatter Reflectometry (OBR) [50] and the possibility to implement a new multiplexing strategy (called scattering-level multiplexing (SLMux) [51]) has driven efforts to develop fibers with different compositions with significantly higher β than conventional telecom optical fibers. MgO nanoparticles have been used as dopants: when deposited in a ring around the core [26], they provided an

extraordinary $\eta_{enh(dB)}$ of 47.5 dB, although with an estimated attenuation of 149 dB/m, which resulted in an approximate $Q_{enh} \sim -300{,}000\ dB$. When the MgO nanoparticles were inserted in the core [52], the authors estimated $\eta_{enh(dB)}$ was 45.2 dB with an attenuation of 17 dB/m, which resulted in $Q_{enh} \sim -34{,}000\ dB$.

The MgO nanoparticle doped fibers were fabricated by MCVD by doping the core with a solution of $MgCl_2$ which was then oxidized. Because of the high processing temperature, alkaline oxides tend to phase separate into particles from a few nm up to hundreds of nm, which then become the main source of Rayleigh scattering, i.e. the largest contributors to η_{enh}. Phase separation of MgO in optical fibers has been shown to be dependent on the dopant concentration [53]: while at low concentrations small nanoparticles are formed, at higher concentrations the nanoparticle sizes are larger than 100 nm. As the nanoparticle refractive index in the near infrared was estimated to be 1.65, significantly higher than that of silica (1.45), 120 nm particles were estimated to induce a loss of 100 dB/m. The authors concluded that sub-50 nm particles need to be used for applications in lasers and amplifiers. Yet, the attenuation seems too high for applications in DOFS.

Calcium-based nanoparticles have also been proposed as dopants for silica fibers [54]: by tailoring nanoparticle distribution size, morphology, and density, fibers with tunable enhanced backscattering in the range of 25.9–44.9 dB have been demonstrated. The reported optical losses were in the range α=50–4350 dB/km, providing a strongly negative Q_{enh} comprised between -74 and -8660 dB.

The combination of commercially available specialty optical fibers and post-fabrication treatments has also been investigated. A photosensitive borogermanosilicate fiber with a high germanium concentration commercialized by Redfern [36] was exposed to the fourth harmonic (at 266 nm) of a Q-switched Nd:YAG laser with 100 mW of power. An FBG was inscribed in the optical fiber by a direct writing scheme at 25 μm/s with a Talbot interferometer and the scattering performance of the fiber was analyzed outside the grating reflection band, providing a $\eta_{enh(dB)}$ ~10 dB. The authors of the research ascribed this to two effects: the presence of dopants that intrinsically increases local nonuniformities (thus Rayleigh scattering) and the large fiber NA which collects more backscattered light. Yet, the presence of high Germanium concentrations and of Boron strongly affects attenuation, thus the overall Q_{enh} is significantly negative.

C. Discrete backscattering

For optical fibers which have been treated post-fabrication, scattering can be locally enhanced in selected areas of the optical fiber core to produce a high scattering contrast between neighboring areas. This is especially useful for sensing specific points along the fiber, or for interference and cavity-based techniques.

In 2013, focused femtosecond laser pulses were used to create cavities in the core of polymer optical fibers [55] that increased backreflection. 120 fs laser pulses at a wavelength of 800 nm with a tunable repetition rate were focused onto a multimode polymethylmethacrylate (PMMA) polymer optical fiber and holes were induced at different exposure parameters. The morphology of the material damage for each pulse was investigated and established to be reproducible for the same settings. A fiber with three reflectors was manufactured and characterized with Optical Time Domain Reflectometry (OTDR), demonstrating the possibility to use this approach for quasi-distributed sensing. The attenuation due to each modification was estimated to be <0.1 dB.

Later, femtosecond laser exposure with high-energy pulses was used to manufacture pairs of scattering structured inside the core of a telecom optical fiber to form an intrinsic Fabry-Perot interferometer for high-temperature sensing. The length of each scattering point was 3 μm, while its cross-sectional area along the fiber longitudinal direction was 2 μm by 2 μm. By adjusting the fabrication conditions, a high fringe visibility of 0.49 and a low insertion loss of 0.002 dB per sensor were achieved [56]. The multiplexed sensor could operate at temperatures as high as 1000 °C and exhibited a sensitivity ranging from 3.71 to 17.15 nm/°C. A DAS system using these optical fibers has been integrated within deep neural networks and both supervised and unsupervised machine learnings were used to identify human movements to achieve >90% identification accuracies [57] and to detect pipeline corrosion and damage classification [58].

Fabry-Perot cavities of enhanced scattering structures inscribed into optical fiber cores by fs laser exposure have demonstrated the possibility to perform high-resolution measurements over a large range of temperatures [59]: an array of 1000 cavities, with -55 dB peak reflectivity and a 100 μm cavity length, written at an interval of 1 mm in a 1 m long telecom optical fiber, exhibited an attenuation as low as 0.0009 dB per cavity, resulting in a maximum multiplexing capacity over 15000. The high-temperature performance of the fibers with Fabry-Perot cavities showed a temperature sensitivity of 18.4 pm/°C at 1000 °C.

Table 1: Comparison of backscattering signal enhancement for different fibers and treatments.

Fibre/treatment	$\eta_{enh(dB)}$ (dB)	Q_{enh} [dB]	Ref.
UV-exposure with hydrogen loading	20	-10	[35]
UV-exposure with hydrogen loading	14		[36]
Fs-laser exposure (800 nm, 300 fs)	16.5		[37]
UV-exposure with hydrogen loading	38	-164	[38]
Ge doped fiber (SM1500)	6.1	-3	[40]
Ge doped fiber (double clad design)	1.3	0.9	[42]
Zirconia nanoparticle doped silica fiber	40	-5540	[47]
MgO nanoparticle doped silica fiber (doping around core)	47.5	-3×10^5	[26]
MgO nanoparticle doped silica fiber (doping in core)	45.2	-3.4×10^4	[52]
Ca-based nanoparticle doped silica fiber	25.9 to 44.9	-74 to -8660	[54]

In summary, enhanced backscattering fibers allow for a stronger backscattered signal which is associated with a significant increase in loss. Table 1 summarizes the backscattering signal enhancement, compared to that of SMF-28 fiber, for various fibers and treatments reported in this

section. Although these fibers are probably unsuitable for significantly extending the range of DOFS, they have found applications in distributed sensing over short lengths, such as OBR in medical applications, where the noise level is substantial.

IV. ENHANCED BACKREFLECTION FIBERS

As discussed above, methods to increase the Rayleigh backscatter often introduce significant propagation loss. On the other hand, enhanced-backreflection fibers (EBRFs) benefit from potentially much smaller loss while maintaining a strong back-reflection signal, due to the directionality offered by the reflector components, thus increasing the light received by the detection system and improving the overall SNR. Despite their operational principle being based on reflection, rather than scattering, for historical reasons, EBRF fibers are still occasionally called "enhanced backscattering fibers". Broadly, EBRFs can be categorized as providing either continuous or discrete backreflection, depending on the density or type of reflectors introduced into the fibre.

A. Continuous backreflection

Many techniques to produce long arrays of continuous and nearly continuous single core gratings have been demonstrated, including point-by-point [35, 66, 67], reel-to-reel [68], encapsulation in a hard shell / drum systems [69], and grating fabrication directly on the drawing-tower [61, 70]. These approaches provide an enhancement of Rayleigh scattering along each point of the fiber, and therefore are suited for high resolution applications.

FBGs have long been used in optical fibers to selectively reflect signals along a narrow wavelength range with high efficiency in a spatially confined section. Several groups have proposed scaling up the fraction of optical fiber covered by FBGs [60, 61] over the whole length of fiber with faint long gratings (FLOG) [62] or continuous gratings [63-65] manufactured using a phase mask, thus producing enhanced-backreflection fibers.

Random gratings written using ultrafast laser point-by-point inscription were reported as a potential candidate for strong EBRFs [71]. A femtosecond Ti:sapphire regenerative amplifier operating at 800 nm was used to deliver 1 μJ, 80 fs pulses with a repetition rate of 100 Hz to the fiber positioned on a high accuracy translation stage. Every single pulse inscribed a grating plane orthogonal to the fiber axis with a thickness smaller than 1 μm by using a cylindrical lens and an objective. A wavelength-division spectral cross-correlation algorithm was used to extract the phase variation induced spectral shift responding to temperature, axial strain, and surrounding refractive index. However, this fiber exhibited very high losses (~100 dB/m), making them impractical for all but very short-range applications.

Another process using fs laser exposure at higher energies demonstrated $\eta_{enh(dB)}$~ 40 dB, but this was achieved by exploiting the formation of nano-gratings in the core of the fiber, which led to a high attenuation of 15 to 41 dB/m [72], corresponding to a maximum Q_{enh} of 10 dB.

An enhancement scheme based on the writing of superimposed linear or chirped FBGs [65, 66] used a reel-to-reel fiber handling system that sent a low-loss optical fiber with a UV-transparent coating to a phase mask, where it was exposed to radiation from a KrF excimer laser delivering ns pulses. The UV pulse fluence is typically a few tens of mJ/cm^2, producing refractive index modulations in the range of 10^{-7} and maintaining the fiber mechanical strength comparable to that of untreated fibers. The fiber, often referred to as "all-grating fiber" was characterized both by OFDR and OBR, which recorded a 20 dB backscatter enhancement with very low optical losses (0.4 dB/km), providing a remarkable overall enhancement of Q_{enh}=19.6 dB. This provided an extremely high enhancement of Rayleigh scattering, although at the expense of spatial resolution: exposure length, typically of the order of a centimeter, limited the achievable spatial resolution to the spacing between each exposure.

Application of this all-grating fiber in conjunction with OFDR for dynamic strain measurement [73] has been investigated, with particular focus on high voltage (1000 kV) spacers [74]: the higher SNR provided by this fiber allowed measurement of the change of strain at the end of a 200 m fiber with a 5 με minimum measurable strain variation and a 10 cm spatial resolution.

A study on the range limitations in all-grating fibers for OFDR sensing found that while measurement of the grating's complex coupling coefficient, from which the sensing measurand is extracted, is substantially impacted by the auto-correlation term, it does not cause a significant error in distributed strain or temperature measurements. The overall sensing range is limited by the breakdown of the Born approximation, i.e. the presence of multiple reflections within very long or strong gratings, [75] but can be increased when there is a spacing between the reflectors [76].

In the approach called ROGUE (Random Optical Grating by Ultraviolet or ultrafast laser Exposure) [40], noise-driven random FBGs were inscribed in an optical fiber at the wavelength where light propagates to produce a wide bandwidth (FWHM >7 nm) independent of grating length, unlike regular FBGs where bandwidth falls inversely with length. The ROGUEs were written using a Talbot interferometer with a phase-mask and a 213 nm laser (the fifth harmonic of a 1064 nm Q-switched laser), with a 100 μm spot size, 30 kHz repetition rate, and 7 ns pulse duration. Because of the noise in the system, the UV exposure was not completely uniform, and a random interference pattern led to enhanced reflectivity over a certain bandwidth determined by the UV fringe patterns. This structure was modeled by the authors as a sequence of short, out-of-phase FBGs that produced a weak reflection grating with a reflectivity that is much higher than typical Rayleigh backscattering over a large bandwidth. The authors estimated an overall enhancement of $\eta_{enh(dB)}$=50 dB with a loss of 0.15 dB/m, resulting in an overall Q_{enh}~ -300 dB. This approach preserved high spatial resolution (at mm level), but compromised on the distance it can operate.

B. *Discrete backreflection*

Long distance applications over many kilometers usually involve the measurement of acoustic signals (DAS) and are performed with a resolution of the order of ten meters. Because of this, Rayleigh scattering enhancement is not required along each point of the fiber, but rather at points positioned at a distance comparable with the DAS system gauge length. This has allowed the manufacture and use of fibers that exhibit the loss of a telecom fiber for >99.99% of its length, and an enhanced backreflection several orders of magnitude larger than an untreated fiber in locations representing less than 0.01% of the fiber length.

Two different approaches have been used to manufacture discrete EBRFs: (1) by inscribing (during fiber drawing) periodic ultra-weak FBGs (UWFBGs) [77, 78], which are wavelength selective, or (2) by introducing (post-fiber fabrication) a series of weak reflectors [79-81], the reflectivity of which is largely wavelength-independent.

These types of fibers have opened a new research field of acoustic sensing where the resolution is defined a-priori by the type of fiber used, called "quasi-distributed acoustic sensing" (QDAS).

1) *Ultra-weak gratings*

The possibility to manufacture FBGs with a single laser pulse [82] was quickly exploited to produce UWFBG arrays in-line, on the drawing tower, during optical fiber manufacturing [83]. This seminal experiment conducted on the drawing tower, used a KrF excimer laser delivering ~ 20 ns pulses with energy in the range 10-40 mJ to an interferometer assembled on the drawing tower: while high energies produced type II gratings with strong reflectivity and 0.5 dB attenuation, low energies produced gratings with 0.2% reflectivity and negligible loss, proving that low loss FBG arrays can be manufactured cheaply and quickly on the drawing tower. The mechanical properties of these draw tower gratings have been shown to be comparable to those of pristine telecom fibers [84-87]. As the single-pulse low reflectivity gratings behave like type I gratings, they tend to work only up to temperatures of ~300 °C. Post-fabrication hydrogen in conjunction with thermal regeneration was used to demonstrate operation at temperatures larger than 800 °C [88].

Because of the challenge of preserving a good alignment over long spans of time, free space interferometers were quickly superseded by transversal interferometrical inscription [89], which used a semi-transparent mirror to split the UV laser beam into two separate beams which were then recombined by three mirrors, and then by a Talbot interferometer [90], which uses a diffractive element for the beam splitting task. The most advanced implementation of in-line Talbot interferometry uses a phase mask as the beam splitter [91], which facilitates interferometer alignment, allows flexibility in the choice of FBG pitch, and minimizes the laser beam energy density on the phase mask during inscription, as a cylindrical lens can then be used after the tiltable mirrors to focus the beam onto the fiber (Fig. 4) [92]. As there is no contact between the interferometric set-up and the optical fiber, this can continuously move along its longitudinal direction.

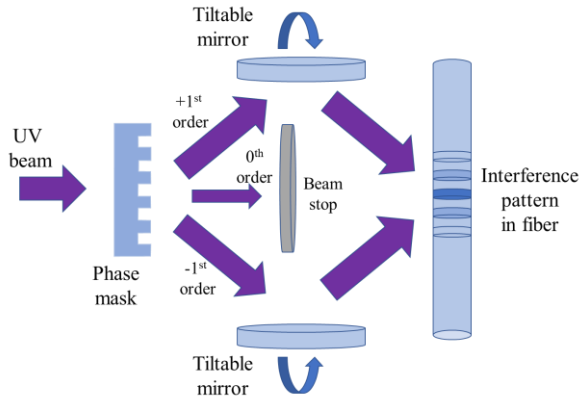

Fig. 4. Fiber grating fabrication using a Talbot interferometer with a phase mask as a diffraction element. The UV laser beam incident on the phase mask is diffracted and the +1 and -1 orders are then incident onto mirrors that interfere them onto the optical fiber. The mirror tilting angle determines the pitch of the interference pattern and thus the Bragg wavelength.

In the draw tower gratings, the strength of each individual FBG is affected by the laser intensity profile, its pulse fluctuations, and pulse width, as well as the transverse and longitudinal vibrations of the optical fiber on the drawing tower. Using the Lorentz-Loren equation, Gladstone-Dale mixing rule, and continuity equation, the refractive index fluctuation along the optical fiber was derived and showed linearity with the gradient of longitudinal vibration velocity [93].

Although the interrogation of multiple FBGs with similar wavelength might seems challenging, the use of Time Division Multiplexing (TDM) [94] has allowed the monitoring of an increasingly larger number of FBGs. More than 1000 ultra-weak FBGs (with peak reflectivity ≤ –37 dB) have been simultaneously probed with this technique [95]. The evaluation of a specific FBG sensor response required a relatively long time as the reflection spectrum of each FBG had to be reconstructed during the entire scanning period in the time domain.

Two optical amplifiers were used in the TDM interrogation system to achieve fast demodulation [96]. A network with 843 FBGs with a peak reflectivity of −40 to −45 dB and a spatial resolution of 2 m was interrogated by 20 ns pulses with a 50 kHz scanning frequency. The authors claim it would be possible to simultaneously interrogate several thousand FBGs in a single optical fiber because of the low crosstalk.

A high-speed high-resolution detection system was implemented using a narrow bandwidth filter to translate wavelength shift measurement into intensity measurement in a network of 342 ultra-weak FBGs with reflectivity of 0.01% and spatial resolution of 2.5 m along an 855 m optical fiber [97]. A reference channel was used to compensate for the source intensity fluctuations. Grating wavelength shifts as little as 0.22 pm at a sampling rate of 100 kHz were measured, providing a 222 nε strain resolution and 2 kHz dynamic frequency.

The use of a double-pulsed optical input waveform with phase demodulation of the differential signals through a heterodyne configuration improved the efficiency of measuring the perturbation by 20 times in comparison to that using a single pulse input [98]. This method was capable of measuring

frequency vibrations as low as 0.2 Hz with a minimum detectable fiber length variation of 14.63 nm.

A serial TDM system was used to interrogate a large-scale sensing network consisting of 1009 identical ultra-weak FBGs with reflectivity of about –33 dB spaced by 2.5 meters from each other [99]. These draw tower FBGs were inscribed in a photosensitive borogermanosilicate optical fiber with an attenuation of α=2.8 dB/km at 1300 nm by using an ArF excimer laser delivering 10 ns pulses with maximum pulse energy of 40 mJ and repetition rate of 300 Hz in combination with an "FBG writing platform" containing a phase mask assembled on the drawing tower. The OTDR trace captured from a fragment of fiber with 200 FBGs allowed the drawing tower fiber attenuation to be estimated at α~10 dB/km. An average reflectivity of 5.67 pW over an injected power of 2.5 nW provided an average reflectivity of -26 dB, a significant improvement with respect to the Rayleigh scattering coefficient (-82 dB) measured in a typical terrestrial telecom fiber [100]. These values provide an overall length enhancement of L_{enh}~ 5.6 km. The same authors showed that the combination of time division multiplexing and wavelength division multiplexing allows for the simultaneous interrogation of 6108 ultra-weak FBGs for temperature monitoring.

Coherent-correlation-OTDR was used for high-resolution quasi-distributed sensing, to interrogate 2000 draw tower gratings in 100 meters of optical fiber to provide a spatial resolution of 50 mm [101].

Drawing tower gratings have been successfully used to increase the operational range of DAS systems in conjunction with ultra-low-loss submarine telecom fibers. A 125 km range was achieved without using inline amplifiers [102]. While this fiber showed promising results for extending the sensing range, beyond 100 km, its relatively high attenuation (α=0.7 dB/km) limits its use to a few kilometers at the far end, where SNR is poor.

It is important to notice that the drawing tower gratings have a bandwidth often only a few nanometers wide. Although this is significantly wider than the Rayleigh backscattering signal of a narrow-line laser or even the bandwidth of a weak grating a few millimeters long (Fig. 5), large temperature changes, vibrations or high pressure might detune the Bragg wavelength out of the detection band, meaning that the reflection signal from the drawing tower FBG will degenerate into Rayleigh scattering, making the sensor essentially ineffective [103]. Indeed, wavelength bandwidths as narrow as 2 nm have been considered for "broadband" weak FBG arrays [104].

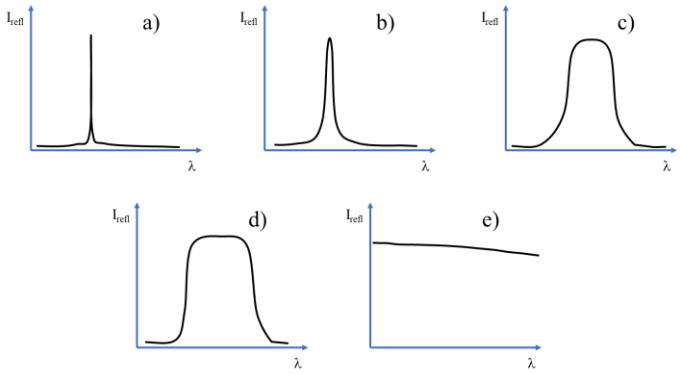

Fig. 5. Schematic of reflection spectra of (a) Rayleigh scattering; (b) a typical 5 mm-long, ultra-weak FBG (UWFBG); (c) a drawing tower grating array; (d) random optical gratings or all-grating fiber; and (e) an ultralow loss enhanced backreflection (ULEB)fiber.

2) Reflector arrays

Although FBGs are considered a mature technology and remarkable results have been achieved with all-grating fibers, their limited operational bandwidth has pushed researchers to develop alternative methodologies that rely on the inscription of series of short reflectors along the fiber. Different types of lasers have been used to write such structures in optical fibers [105]; yet, femtosecond lasers have quickly become the laser of choice because they have been the most successful to produce low-loss reflectors.

In particular, by scanning focused fs laser pulses it is possible to induce a smooth refractive index increase (without scattering damage or nanograting formation) localized at the beam focus path. A wide range of glasses can be processed since the material modification mechanism relies on multiphoton absorption, which does not require glass photosensitivity, unlike UV inscription methods. An example of an OTDR trace for a typical fs-laser written reflector fiber is given in Fig. 6, which shows high reflectance points spaced every 10 m over the fiber's intrinsic Rayleigh backscatter baseline.

Reflector arrays have been employed with particular success for long-range distributed acoustic sensing based on phase-optical time domain reflectometry (φ-OTDR), in which the phase difference variation between the backreflected light from two given adjacent reflectors is proportional to the strain change within that fiber section. A key advantage is that backreflections occur at discrete points, unlike traditional φ-OTDR which uses Rayleigh backscattering arising from extended regions (the length of which depend on the probe pulse duration), and hence this approach improves linearity of the strain-phase response and minimizes interference fading, leading to lower phase noise.

In 2018, a femtosecond laser was used to modify the core refractive index of a telecom optical fiber to increase the Rayleigh signal by up to $\eta_{enh(dB)}$=17 dB [106] without inducing any physical damage. A standard telecoms fiber, with an attenuation of 0.2 dB/km, was exposed to radiation from a frequency doubled solid state Yb:KGW laser delivering ~3 μJ 200 fs pulses at the wavelength 515 nm. In the visible, the fiber polymer coating is transparent, thus its removal prior to inscription was unnecessary.

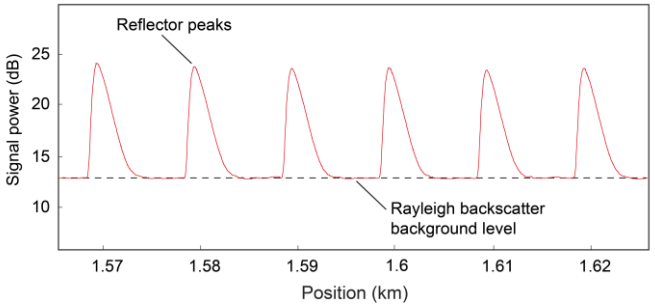

Fig. 6. Typical reflection response of ULEB fiber from a commercial OTDR system (EXFO OTDR machine MAX-715B-M2-EA) operating with 5 ns pulses at the 1550 nm wavelength. Reflectors are spaced at 10 m intervals and have a standard deviation of 0.9 dB. In typical DOFS operation using phase-OTDR, the reflected signal phase variations between adjacent reflectors are analyzed in order to determine environmental changes such as vibrations over that section of fiber.

A semi-automated reel-to-reel system (Fig. 7) was used to inscribe 27 reflectors into the fiber and OTDR was used to monitor the backscattered signal. Optical Side Scattering Radiometry (OSSR) measurements revealed an attenuation amounting to 0.3 dB/km if reflectors were placed every 1 m along the fiber. Because of the extremely low loss associated with this technique, the fibers were called ultra-low-loss enhanced backreflection (ULEB) fibers. Unlike FBGs, this type of optical fiber provides a broadband reflectivity spectrum (Fig. 5e) with a bandwidth often in excess of 150 nm, meaning that they are unaffected by large temperature or strain variations.
In 2019, an array of 49 reflectors with −40 dB reflectivity and at 20 m intervals was also manufactured by fs laser exposure and used for improving the SNR of a DAS system using phase-noise compensation and pulse compression. Experiments with a 20 km link loss showed that the system noise level was −93.16 dB (re rad/√Hz), corresponding to a strain resolution of 92.84 fε/√Hz, in the frequency range 500–2500 Hz [107]. Yet, the transmission loss of this optical fiber was high (1.1 dB/km) [108], thus unsuitable for sensing at ultra-long distances. This approach was improved to manufacture one thousand weak reflectors with an interval of 10 m and a reflectivity around −42 dB to provide an optical fiber attenuation of 0.34 dB/km and $\eta_{enh(dB)}$ of 15.8 dB, yielding a Q_{enh} of 15 dB [108]. These parameters provide an extension of operational length for a DAS system of L_{enh}~23 km.

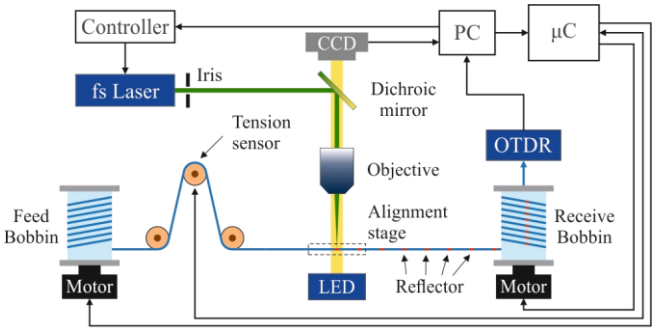

Fig. 7. Reel-to-reel reflector inscription system. A femtosecond (fs) laser, driven by a controller, delivers pulses to an objective that focuses the beam into the optical fiber. A CCD is used to monitor the relative position of the fiber, which is driven across the writing stage by motors. A PC collects information from the CCD camera and from the OTDR system, which is used to drive the motors (through a microcontroller) and the fs laser (through a controller). An optical time-domain reflectometer (OTDR) is added to monitor the reflectivity of the reflectors in real-time. A micro-controller (µC) is used to control the operation of the feeding and receiving reels [116].

Further improvements allowed a decrease in the loss even further, with an attenuation of 0.0001 dB per reflector [109], meaning that an ULEB fiber with 100 reflectors spaced every 10 m would exhibit an attenuation of 0.21 dB/km, only ~5% higher than the value quoted by manufacturers of conventional terrestrial telecom optical fibers. An ULEB fiber with a set of 10 reflectors with a reflectance of −53 dB was used for acoustic sensing and enabled an average phase noise of −91 dB (re rad^2/Hz), two orders of magnitude lower than that observed in sensors formed using Rayleigh backscattering in the same fiber [109]. More importantly, the sensor exhibited excellent (>50 dB) non-local signal suppression, a high degree of linearity, and was immune to interference fading. Assuming a $\eta_{enh(dB)}$ of 29 dB, such a fiber can provide a quality factor enhancement of Q_{enh}= 28.6 dB and a staggering length extension of L_{enh}=69 km.

An investigation into the optimal arrangement of reflectors in a standard telecommunication fiber [110] found that the maximum operating range of distributed sensors based on φ-OTDR utilizing probe pulses with a duration of 200 ns can be increased by 53 km using ultra-low-loss fiber with an attenuation of 0.16 dB/km, thereby extending it to 173 km without using distributed, remotely pumped, or in-line amplifiers. This is larger than the 140 km predicted for the all-grating fiber with chirped FBGs [111].

A frequency multiplexed interrogator was used to interrogate an ULEB containing up to 1000 point reflectors over 10 km to increase the effective pulse repetition rate by one order of magnitude [112]. Four fiber sections each 2.5 km long with reflectors spaced 10 m apart and mean reflectivity values between -48 dB and -63 dB have been investigated, as shown in Fig. 8.

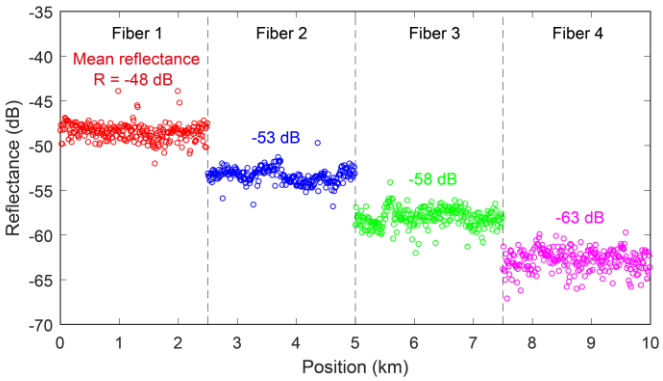

Fig. 8. Reflectance plot of 10 km ULEB fibre with 1000 reflectors, formed by 4 fiber sections with 250 reflectors each targeting reflectance values between -63 to -48 dB, used for distributed acoustic sensing by phase OTDR in [112].

The phase noise was lowest for the fiber sections with the highest reflector strength and reached a minimum of −101 dB (re rad^2/Hz) for the -48 dB reflectors, corresponding to a strain noise of 0.095$p\varepsilon$/√Hz. Furthermore, the use of frequency multiplexing with 10 different frequency probe pulses

temporally spaced evenly allowed a tenfold increase in sensor bandwidth – this was possible as the frequency diversity was no longer needed to correct for interference fading as in the case of Rayleigh backscatter based schemes.

The use of ULEB fibers can eliminate the need for averaging, allowing single-shot operation [113, 114]. A distributed dynamic strain sensing system based on frequency-scanning φ-OTDR and an RF pulse scheme with a fast arbitrary waveform generator was used in conjunction with an ULEB fiber to demonstrate a 20 cm spatial resolution, 60 με strain range, and 27.8 kHz sampling rate in a 55 m long fiber and 60 frequency steps. The strain noise floor was <1.8 nε/√Hz for vibrations below 700 Hz and <0.7 nε/√Hz at higher frequencies. Using a single shot coherent OTDR [114], 2.3 pε/√Hz was demonstrated over a 134 m long fiber with 2 m spatial resolution, and a strain sensitivity of better than 100 pε/√Hz on a 75 km fiber.

A high sensitivity and large measurable strain range DAS scheme was demonstrated using a sub-chirped-pulse extraction algorithm (SPEA) in the time domain [115]. When the ULEB fiber was used, an 80.7 pε/√Hz strain sensitivity with 28.4 cm spatial resolution was achieved over a length of 920 m. A 60 με strain range was observed during a single-shot measurement.

ULEB fibers were exploited to improve the spatial resolution of DAS systems using a φ-OTDR system to 10 cm [116]. Importantly, the use of backreflections from ULEB fibers overcomes the trade-off between the spatial resolution and SNR, which Rayleigh backscatter-based methods suffer from (a longer pulse gives a stronger Rayleigh backscatter signal, but physically occupies a longer length thus impairing resolution). The ULEB fiber with 50 reflectors having an average reflectance of −56 dB was fabricated with an automated reel-to-reel inscription machine. The phase noise was measured to be 1.9 $n\varepsilon/\sqrt{Hz}$ over the 1 km sensing range.

ULEB fibers in combination with in-line optical amplification were exploited to extend the DAS range from a single access point beyond 152 km [117]. The sensing system was capable of quantifying vibrations at the far end with a minimum detectable strain of 40 nε at 1 Hz. The DAS system operated within the frequency range of 0.1–100 Hz with a maximum spatial resolution of 5 m. The authors believed that the sensing range could be extended beyond 200 km by using ultra-low-loss submarine telecom fibers and increasing the ULEB fiber length. A model was developed to account for components noise and imperfection in a DAS system including ULEB fibers [118].

ULEB fibers have also been used for sensing with low-coherence sources to detect vibrations with frequencies up to 1 kHz and strain resolution of 50 $p\varepsilon/\sqrt{Hz}$ without observable cross-talk [119]. The ULEB fiber had -40 dB reflectors spaced 20 m apart and frequency-shifted interferometry was used in the DAS system with a low coherence light source to locate the position of the vibration.

Networks of ultrahigh resolution strain sensing using identical ULEB fibers free of strain as reference were used for compensating the ultra-low frequency noise in the φ-OTDR system [120]. Residual errors arising from thermal hysteresis nonlinearity between the sensing and reference fibers were reduced by using a hysteresis operator based least squares support vector machine model, which effectively compensated the phase bias drift with frequency below 0.1. The proposed strain sensor network exhibited a high dynamic resolution of 10.5 pε/√Hz above 10 Hz, and an ultra-low frequency sensing resolution of 166 pε at 1 mHz.

To further improve the performance, multiplexing in the frequency domain could be used: multiple-input–multiple-output (MIMO) technology, frequently used in telecoms and radar systems, has produced a 4.6 pε/√Hz strain sensitivity and 5 m spatial resolution [121] when using UWFBGs and the authors claim this could be easily deployed with ULEB optical fibers.

ULEB fibers were used with OFDR for increased spatial resolution measurements: using an inexpensive tunable laser diode with a 1 nm tuning range and an ULEB fibers with over 40 dB enhancement reflectors spaced by 4.8 cm, strain measurements with a root mean square accuracy of fewer than 2.70 με were achieved when 10–50 με was exerted to the sensing fiber [122]. An ULEB fiber containing 48 reflectors with a reflectivity level of -50.5 dB spaced by 20 cm was interrogated with a commercial Luna OBR 4600 OFDR system [123], tuning over 10 THz at 25 THz/s, resulting in a DAS with 0.02 rad phase noise, 24 kHz range with 2.32 Hz sample spacing.

The combination of OFDR and φ-OTDR in ULEB fibers was proposed for the calculation of absolute values of displacement of artificial reflecting points: for a 110 ns pulse duration and 10 Hz frequency, the distance between two reflectors measured by the method was 9.84 ± 0.04 m with 0.16 μm accuracy of relative measurements [124].

To increase the acoustic sensitivity in air, a hollow cylinder was used for acoustic wave transduction [125]. Coherent phase detection was used to realize high-fidelity recovery of the airborne sound wave, providing a phase sensitivity of −112.5 dB (re 1 rad/μPa) within the frequency range of 500 Hz–5 kHz and a peak sensitivity up to −83.7 dB (re 1 rad/μPa) at 80 Hz.

The same configuration with an ULEB fiber wrapped around a cylinder has been used to monitor liquid levels [126] with a 142 μm sensing resolution. The authors claim that the proposed liquid level sensor has a potential sensing range of 320 m with no resolution degeneration in theory, corresponding to a 127 dB sensing dynamic range.

Reflector arrays have found applications outside distributed sensing, in particular in fiber laser cavities [127], which can provide a better strain sensitivity than regular FBGs, or random lasers [128].

V. CONCLUSIONS

In the last decade, numerous approaches have been investigated to increase the SNR in optical fibers exploiting Rayleigh scattering for sensing.

While enhanced backscattering fibers are being explored for short distance applications which require a strong signal or operate in a very noisy environment, such as medical sensing, enhanced backreflection fibers have gained increased interest

for DOFS systems.

The use of all-grating fibers (drawing tower gratings or ultraweak FBGs) seems attractive for applications where wavelength encoding is important, such as distributed temperature and/or strain systems. The limited reflection bandwidth (often smaller than 10 nm) might limit the sensor dynamic range, though.

The use of reflector arrays, in particular, is promising for future applications in DAS as their strong signal enhancement (often >20 dB larger than the Rayleigh backscatter) is combined with an extremely broadband operational wavelength bandwidth and minimal additional attenuation with respect to telecom fibers (of the order of 0.01 dB/km for 10 m reflector spacing). They have a strong potential to extend the operational range of DAS systems to distances well exceeding 200 km from a single access.

Despite the clear benefits they bring in terms of enhanced SNR and sensing distance, in comparison to commercial fibers enhanced backreflection fibers still have a relatively high cost, require additional postprocessing after fiber drawing, and are not widely available commercially. Novel structures, such as quasi-distributed reflector pairs might provide the possibility to reap the benefits of a low-loss fiber and some wavelength encoding capabilities.

Finally, it is important to note that although different types of specialty optical fibers can provide an enhanced response to strain and temperature, the DOFS response to external stimuli ultimately has a strong dependence on coatings and cabling [129-130], which in fact provide both a large cross section for the interaction with strain fields and a transfer medium [131-135].

REFERENCES

[1] H. C. Lefevre, "*The Fiber-Optic Gyroscope*," 3rd ed., Artech House Ed., Norwood, MA, USA, 2022.

[2] R. Kashyap, "*Fiber Bragg gratings*," 2nd ed., Academic Press, Burlington, MA, USA, 2009.

[3] A. H. Hartog, "*An Introduction to Distributed Optical Fibre Sensors*," CRC press, Boca Raton, FL, USA, 2017.

[4] J. Li, M. Zhang, "Physics and applications of Raman distributed optical fiber sensing," *Light Sci Appl.*, Vol. 11, art. 128 , May 2022.

[5] A. Motil, A. Bergman, M. Tur, "State of the art of Brillouin fiber-optic distributed sensing" *Opt. Las. Technol.*, Vol. 78, Part A, pp. 81-103, Apr. 2016.

[6] L. Palmieri, L. Schenato, M. Santagiustina, A. Galtarossa, "Rayleigh-Based Distributed Optical Fiber Sensing", *Sensors*, Vol. 22, no. 18, 6811, Sep 2022.

[7] P. Lu *et al.*, "Distributed optical fiber sensing: Review and perspective", *Appl. Phys. Rev.*, Vol. 6, no. 4, 041302, Sep 2019.

[8] A. Ukil, H. Braendle, P. Krippner, "Distributed Temperature Sensing: Review of Technology and Applications." *IEEE Sens. J.*, Vol. 12, no. 5, pp. 885–892, May 2012.

[9] Z. Amira, M. Bouyahi, T. Ezzedine, "Measurement of Temperature through Raman Scattering." *Procedia Computer Sci.*, Vol. 73, pp. 350–357, Dec. 2015.

[10] A. Masoudi, T. Newson, "Contributed Review: Distributed optical fibre dynamic strain sensing," *Rev. Sci. Instr*., Vol. 87, 011501, Jan 2016.

[11] C.A. Galindez-Jamioy, J.M. López-Higuera, "Brillouin Distributed Fiber Sensors: An Overview and Applications." *J. Sens.* Vol. 2012, 204121, Oct. 2012.

[12] D.J.J. Hu, *et al.*, "Review of Specialty Fiber Based Brillouin Optical Time Domain Analysis Technology." *Photonics*, Vol. 8, no.10, pp. 421, Sep. 2021,

[13] X. Bao, Y. Wang "Recent Advancements in Rayleigh Scattering-Based Distributed Fiber Sensors," *Adv. Dev. Instrum.*, Vol. 2021, 8696571, Mar 2021.

[14] L. Palmieri *et al.*, "Rayleigh-Based Distributed Optical Fiber Sensing," *Sensors*, Vol. 22, 6811, Sep 2022.

[15] I. Floris *et al.*, "Fiber Optic Shape Sensors: A comprehensive review," *Opt. Lasers Eng.*, Vol. 139, 106508, Apr 2021.

[16] A.J. Rogers, "Distributed Optical-Fibre Sensors for the Measurement of Pressure, Strain and Temperature." *J. Inst. Electron. Radio Eng.*, Vol. 58, S113–S122, Oct. 1988.

[17] A.J. Rogers, "Polarization-optical time domain reflectometry: a technique for the measurement of field distributions," *Appl. Opt.*, vol. 20, pp. 1060–1074, Mar. 1981.

[18] M. Olivero *et al.*, "Distributed X-Ray Dosimetry with Optical Fibers by Optical Frequency Domain Interferometry," *IEEE Trans. Instrum. Meas.*, vol. 70, 7003909, Apr. 2021.

[19] Z. He, Q. Liu, "Optical Fiber Distributed Acoustic Sensors: A Review." *J. Light. Technol.*, vol. 39, no. 12, pp.3671–3686, Jun. 2021.

[20] A. Masoudi, M. Belal, and T. P. Newson. "A distributed optical fibre dynamic strain sensor based on phase-OTDR." *Meas. Sci. Technol.* Vol. 24, 085204, 2013.

[21] O.H. Waagaard *et al.*, "Real-time low noise distributed acoustic sensing in 171 km low loss fiber," *Continuum*, vol. 4, no. 2, pp. 688-701, Feb. 2021

[22] Y. Dang, *et al.*, "Simultaneous distributed vibration and temperature sensing using multicore fiber." *IEEE Access*, vol. 7, pp. 151818-151826, Oct 2019.

[23] A. Coscetta *et al.*, "Distributed Static and Dynamic Strain Measurements in Polymer Optical Fibers by Rayleigh Scattering," *Sensors*, Vol. 21, 5049, Jul. 2021.

[24] M. Chen, A. Masoudi, F. Parmigiani, and G. Brambilla, "Distributed acoustic sensor based on a two-mode fiber," *Opt. Express*, vol. 26, no. 19, pp. 25399-25407, Sep. 2018.

[25] Matthew J. Murray, Allen Davis, and Brandon Redding, "Multimode fiber Φ-OTDR with holographic demodulation," *Opt. Express*, vol. 26, no. 18, pp. 23019-23030, Aug. 2018.

[26] T. Ayupova *et al.*, "Fiber optic refractive index distributed multi-sensors by scattering-level multiplexing with MgO nanoparticle-doped fibers," *IEEE Sensors J.*, vol. 20, no. 5, pp. 2504–2510, Mar. 2020.

[27] H. Kanamori, "Transmission Loss of Optical Fibers; Achievements in Half a Century", *IEICE Transactions on Communications*, vol. E104.B, no. 8, pp. 922-933, Aug. 2021.

[28] Y. Tamura *et al.*, "The First 0.14-dB/km Loss Optical Fiber and its Impact on Submarine Transmission". *IEEE J. Lightwave Technol.*, Vol. 36, no. 1, pp. 44-49, Jan 2018

[29] G.T. Jasion *et al.*, "0.174 dB/km Hollow Core Double Nested Antiresonant Nodeless Fiber (DNANF)", 2022 Optical Fiber Communications Conference and Exhibition (OFC), pp.1-3, Mar 2022.

[30] A. Q. Tool "Relation between inelastic deformability and thermal expansion of glass in its annealing range," *J. Amer. Ceramic Soc.*, vol. 29, no. 9, pp. 240–253, Sep. 1946.

[31] S. Sakaguchi, "Relaxation of Rayleigh scattering in silica core optical fiber by heat treatment," *Electron. Commun. Jpn.*, vol. 83, no. 12, pp. 35–41, Nov. 2000.

[32] M. E. Lines, "Can the minimum attenuation of fused silica be significantly reduced by small compositional variations? I.Alkali metal dopants," *J. Non-Cryst. Solids*, vol. 171, pp. 209–218, Aug. 1994.

[33] M. E. Lines "Can the minimum attenuation of fused silica be significantly reduced by small compositional variations? II. Combined fluorine and alkali metal dopants," *J. Non-Cryst. Solids*, vol. 171, pp. 219–227, Aug. 1994.

[34] D. Johlen *et al.*, "UV-induced absorption, scattering and transition losses in UV side-written fibers." *Opt. Fiber Comm. Conf.*, Optica Publishing Group, Mar. 1999.

[35] S. Loranger *et al.*, "Rayleigh scatter based order of magnitude increase in distributed temperature and strain sensing by simple UV exposure of optical fibre," *Sci. Rep.*, vol. 5, no. 1, 11177, Sep. 2015.

[36] F. Parent *et al.*, "Enhancement of accuracy in shape sensing of surgical needles using optical frequency domain reflectometry in optical fibers," *Biomed. Opt. Express*, vol. 8, no. 4, pp. 2210–2221, Mar. 2017.
[37] M. Wang *et al.*, "Ultrafast laser enhanced Rayleigh backscattering on silica fiber for distributed sensing under harsh environment." Conference on Lasers and Electro-Optics (CLEO), May 2018.
[38] F. Parent *et al.*, "Intra-arterial image guidance with optical frequency domain reflectometry shape sensing," *IEEE Trans. Med. Imag.*, vol. 38, no. 2, pp. 482–492, Feb. 2019.
[39] B. Szczupak *et al.*, "The influence of germanium concentration in the fiber core on temperature sensitivity in Rayleigh scattering-based OFDR." *IEEE Sensors J.*, Vol. 21, no.18, pp. 20036-20044, Sep. 2021.
[40] F. Monet *et al.*, "The ROGUE: A novel, noise-generated random grating," *Opt. Express*, vol. 27, no. 10, pp. 13895–13909, May 2019
[41] https://fibercore.humaneticsgroup.com/products/photosensitive-fiber/highly-germanium-doped-fiber/sm15004250.
[42] M.-J. Li, S. Li, and J. S. Stone, "Novel optical fibers for distributed sensor applications," in *Proc. 25th Int. Conf. Opt. Fiber Sensors*, Jeju, South Korea, pp. 1–4, Apr. 2017.
[43] M. T. Reaves *et al.*, "Optical fiber and method and apparatus for accurate fiber optic sensing under multiple stimuli," U.S. Patent 3 218 747 B1, Nov. 2020.
[44] M. E. Froggatt *et al.*, "Dissimilar cores in multicore optical fiber for strain and temperature separation," U.S. Patent 10 132 614 B2, Nov. 2018.
[45] W. Blanc, B. Dussardier, "Formation and applications of nanoparticles in silica optical fibers." *J Opt.*, vol. 45, pp. 247–254, oct. 2016.
[46] P. Bulot, *et al.*, "OFDR distributed temperature sensing at 800°C on a fiber with enhanced Rayleigh scattering profile by doping," in Advanced Photonics 2018 (BGPP, IPR, NP, NOMA, Sensors, Networks, SPPCom, SOF), OSA Technical Digest, paper BM3A.2, Jul. 2018.
[47] P. Bulot *et al.*, "Performance Study of a Zirconia-Doped Fiber for Distributed Temperature Sensing by OFDR at 800 °C", *Sensors*, vol. 21, no. 11, pp. 3788, May 2021
[48] X. Wang, R. Benedictus, and R. M. Groves, "Optimization of light scattering enhancement by gold nanoparticles in fused silica optical fiber," *Opt. Express*, vol. 29, no. 13, pp. 19450-19464, June 2021.
[49] X. Wang, R. Benedictus, and R.M. Groves "Spectral characteristics of gold nanoparticle doped optical fibre under axial strain." *Sci Rep.*, vol. 12, 16593, oct. 2022.
[50] M. Froggatt and J. Moore, "High-spatial-resolution distributed strain measurement in optical fiber with Rayleigh scatter," *Appl. Opt.*, vol. 37, no. 10, pp. 1735–1740, Apr. 1998.
[51] A. Beisenova *et al.*, "Simultaneous distributed sensing on multiple MgO-doped high scattering fibers by means of scattering-level multiplexing," *J. Lightwave Technol.*, vol. 37, no. 13, pp. 3413–3421, Jul. 2019.
[52] A. Beisenova *et al.*, "Distributed fiber optics 3D shape sensing by means of high scattering NP-doped fibers simultaneous spatial multiplexing," *Opt. Express*, vol. 27, no. 16, pp. 22074–22087, Aug. 2019.
[53] W. Blanc, *et al.*, "Fabrication of rare earth-doped transparent glass ceramic optical fibers by modified chemical vapor deposition," *J. Am. Ceram. Soc.*, vol. 94, no.8, pp. 2315-2318, May 2011.
[54] V. Fuertes *et al.*, "Engineering nanoparticle features to tune Rayleigh scattering in nanoparticles-doped optical fibers," *Sci. Rep.*, vol. 11, 9116, Apr. 2021.
[55] S. Liehr *et al.*, "Femtosecond laser structuring of polymer optical fibers for backscatter sensing," *J. Lightwave Technol.*, vol. 31, no. 9, pp. 1418–1425, May 2013.
[56] M. Wang *et al.*, "Multiplexable high-temperature stable and low-loss intrinsic Fabry-Perot in-fiber sensors through nanograting engineering." *Opt. Express*, vol. 28, no. 14, pp. 20225-20235, Jun. 2020.
[57] Z. Peng *et al.*, "Fiber-optical distributed acoustic sensing signal enhancements using ultrafast laser and artificial intelligence for human movement detection and pipeline monitoring," in *Optical Data Science II* (International Society for Optics and Photonics, 2019), p. 109370J.
[58] Z. Peng, *et al.*, "Distributed fiber sensor and machine learning data analytics for pipeline protection against extrinsic intrusions and intrinsic corrosions." *Opt. Express*, vol. 28, no. 19, pp. 27277-27292, Sep. 2020.
[59] B. Du *et al.*, "High-Density Weak In-Fiber Micro-Cavity Array for Distributed High-Temperature Sensing with Millimeter Spatial Resolution." *J. Lightwave Technol.*, vol. 40, no. 22, pp. 7447-7455, Aug. 2022.
[60] C. G. Askins *et al.*, "Stepped-wavelength optical-fiber Bragg grating arrays fabricated in line on a draw tower", Opt. Lett., vol. 19, no.2, pp. 147-129, Jan. 1994.
[61] W. Bai *et al.*, "All fiber grating (AFG): a new platform for fiber optic sensing technologies", International Conference on Optical Fibre Sensors (OFS24) in *Proc. SPIE*, vol. 9634, 96342A, Sep. 2015.
[62] L. Thévenaz et al., "Novel technique for distributed fibre sensing based on faint long gratings (FLOGs)," Proc. SPIE 9157, 23rd International Conference on Optical Fibre Sensors, 91576W, Jun. 2014.
[63] M. Gagné *et al.*, "Fabrication of high quality ultra-long fiber Bragg gratings: Up to 2 million periods in phase", *Opt. Exp.*, vol. 22, no. 1, pp. 387-398, 2014.
[64] P. S. Westbrook *et al.*, "Kilometer length, low loss enhanced back scattering fiber for distributed sensing", *Proc. 25th Opt. Fiber Sensors Conf. (OFS)*, pp. 1-5, Apr. 2017.
[65] P. S. Westbrook *et al.*, "Improving distributed sensing with continuous gratings in single and multi-core fibers", *Proc. Opt. Fiber Comm. Conf.*, pp. 1-3, Mar. 2018.
[66] P. S. Westbrook *et al.*, "Continuous multicore optical fiber grating arrays for distributed sensing applications," *J. Lightwave Tech.*, Vol. 35, no. 6, pp. 1248–1252, Mar. 2017.
[67] A. Asseh *et al.*, "A writing technique for long fiber Bragg gratings with complex reflectivity profiles," *J. Lightwave Tech.*, vol. 15, no. 8, pp. 1419–1423, Aug. 1997.
[68] P. Lefebvre *et al.*, "Automated manufacturing of fiber Bragg grating arrays," in *Proc. Opt. Fiber Sens. Conf.*, ThE27, 2006.
[69] J. F. Brennan *et al.*, "Dispersion correction with a robust fiber grating over the full C-band at 10-Gb/s rates with <0.3-dB power penalties," *IEEE Photon. Technol. Lett.*, vol. 15, no. 12, pp. 1722–1724, Dec. 2003.
[70] C. G. Askins *et al.*, "Stepped wavelength optical-fiber Bragg grating arrays fabricated in line on a drawing tower," *Opt. Lett.*, vol. 19, no. 2, pp. 147–149, Jan. 1994.
[71] Y. Xu *et al.*, "Optical fiber random grating-based multiparameter sensor," *Opt. Lett.*, Vol. 40, no. 23, pp. 5514–5517, Nov. 2015.
[72] A. Yan *et al.*, "Distributed Optical Fiber Sensors with Ultrafast Laser Enhanced Rayleigh Backscattering Profiles for Real-Time Monitoring of Solid Oxide Fuel Cell Operations," *Sci. Rep.*, Vol. 7, no. 1, pp. 9360, 2017.
[73] C. Wang *et al.*, "High sensitivity distributed static strain sensing based on all grating optical fiber in optical frequency domain reflectometry." In *Advanced Sensor Systems and Applications XI*, Vol. 11901, pp. 61-67, Oct. 2021.
[74] W. Qin *et al.*, "A Distributed Strain Measurement Method for Ultra-high Voltage GIL Spacer Based on OFDR and All Grating Fiber." In *Optical Fiber Sensors*, pp. T3-28, Jun. 2020.
[75] J. D. Hart, C. R. S. Williams, and G. A. Cranch, "Range limitations of optical frequency domain reflectometry with all-grating fiber for distributed strain and temperature sensing," *Opt. Express*, vol. 29, no. 26, pp. 44300-44315, Dec. 2021.
[76] J.D. Hart, M.N. Hutchinson, and G.A. Cranch, "Comparison of all-grating fiber and enhanced backscatter fiber for distributed strain sensing" In *Optical Fiber Sensors* (pp. T1-5), Jun 2020
[77] F. Ai *et al.*, "Wideband Fully-Distributed Vibration Sensing by Using UWFBG Based Coherent OTDR." *Proc. Opt. Fib. Comm. Conf.*, Los Angeles, CA, USA, p. W2A.19, Mar. 2017.
[78] J.B. Huang *et al.*, "Progress in Fabrication, Demodulation and Application of Weak-Reflection Fiber Bragg Grating Array." *Laser Optoelectron. Prog.* Vol. 58, 1700005, 2021.
[79] M. Wu *et al.*, "Frequency Response Enhancement of Phase-Sensitive OTDR for Interrogating Weak Reflector Array by Using OFDM and Vernier Effect." *J. Light. Technol.*, Vol. 38, no. 17, pp. 4874–4882, Sep. 2020.
[80] K. Hicke, R. Eisermann, S. Chruscicki, "Enhanced Distributed Fiber Optic Vibration Sensing and Simultaneous Temperature Gradient Sensing Using Traditional C-OTDR and Structured Fiber with Scattering Dots." *Sensors*, Vol. 19, no. 19, pp. 4114, Sep. 2019.
[81] B. Redding *et al.*, "Low-noise distributed acoustic sensing using enhanced backscattering fiber with ultra-low-loss point reflectors." *Opt. Express*, Vol. 28, no. 10, pp. 14638–14647, May 2020.

[82] C.G. Askins *et al*., "Fiber Bragg reflectors prepared by a single excimer pulse," *Opt.Lett.*, vol. 17, no. 11, pp. 833-835, Jun. 1992

[83] L. Dong *et al*., "Single pulse Bragg gratings written during fibre drawing." *Elctron.Lett.*, vol. 29, no. 17, pp. 1577-1578, Aug. 1993

[84] C.G. Askins *et al.,* "Fiber strength unaffected by on-line writing of single-pulse Bragg gratings," *Electron. Lett.*, vol. 33, no. 15, pp. 1333-1334, Jul. 1997.

[85] V. Hagemann *et al.*, "Mechanical resistance of draw-tower-Bragg-grating Sensors," *Electron. Lett.*, vol. 34, no. 2, pp. 211-212, Jan. 1998

[86] P. Mauron *et al*., "Lifetime of Fibre Bragg Gratings Under Cyclic Fatigue" in *Proc. Conf. on Optical Fiber Reliability and Testing*, Boston, Massachusetts, USA, 1999, pp. 1-9.

[87] M.W. Rothhardt, "High mechanical- strength single-pulse draw tower gratings," *Proc. SPIE 5579, Photonics North 2004: Photonic Applications in Telecommunications, Sensors, Software, and Lasers*, 2004, pp. 127-135.

[88] E. Lindner *et al.*, "Post-hydrogen-loaded draw tower fiber Bragg gratings and their thermal regeneration," *Appl. Opt.*, vol. 50, no.17, pp. 2519-2522, Jun. 2011.

[89] C.G. Askins *et al.*, "Stepped wavelength optical fiber Bragg grating arrays fabricated in line on a draw tower." *Opt. Lett.*, vol. 19, no. 2, pp. 147-149, Jan. 1994.

[90] C. Chojetzki *et al.*, "High-reflectivity draw-tower fiber Bragg gratings—arrays and single gratings of type II." *Opt. Eng.*, vol. 44, no. 6, 060503, Jun. 2005.

[91] H. Bartelt *et al.*, "Single-pulse fiber Bragg gratings and specific coatings for use at elevated temperatures," *Appl. Opt.*, vol. 46, no.17, pp. 3417-3424, May 2007.

[92] A.I. Gribaev, *et al.*, "Laboratory setup for fiber Bragg gratings inscription based on Talbot interferometer." *Optical and Quantum Electronics*, vol. 48, no. 12, pp 1-7, Nov. 2016.

[93] H. Guo *et al.*, "Ultra-weak FBG and its refractive index distribution in the drawing optical fiber," *Opt. Express*, vol. 23, no. 4, pp. 4829-4838, Feb. 2015.

[94] D.J. Cooper, T. Coroy, and P.W. Smith, "Time-division multiplexing of large serial fiber-optic Bragg grating sensor arrays." *Appl. Opt.*, vol. 40, no. 16, pp. 2643-2654, Jun. 2001.

[95] Y. Wang *et al.*, "A large serial time-division multiplexed fiber Bragg grating sensor network," *J. Lightwave Tech.*, vol. 30, no. 17, pp. 2751–2756, Sep. 2012.

[96] C. Hu, H. Wen, and W. Bai, "A Novel Interrogation System for Large Scale Sensing Network With Identical Ultra-Weak Fiber Bragg Gratings," *J. Lightwave Technol.*, vol. 32, no. 7, pp. 1406-1411, Apr. 2014.

[97] P. Han et al., "A High-Speed Distributed Ultra-Weak FBG Sensing System With High Resolution," *Photon. Technol. Lett.*, vol. 29, no. 15, pp. 1249-1252, Aug 2017.

[98] L. Ma *et al.*, "High-Speed Distributed Sensing Based on Ultra Weak FBGs and Chromatic Dispersion," *Photon. Technol. Lett.*, vol. 28, no. 12, pp. 1344-1347, Jun. 2016,

[99] M. Yang *et al.*, "Huge capacity fiber-optic sensing network based on ultra-weak draw tower gratings." *Photonic Sensors*, vol. 6, no.1, pp. 26-41, Dec. 2016.

[100] Corning® SMF-28e+® Photonic Optical Fiber datasheet, M1100025, Mar 2010.

[101] F. Azendorf *et al*., "Interrogation of 2000 Draw Tower Gratings for Quasi Distributed Sensing with Coherent-Correlation-OTDR." In *Optical Sensors*, pp. SM2C-3, Jul. 2022.

[102] G. Cedilnik *et al*., "Pushing the Reach of Fiber Distributed Acoustic Sensing to 125 km Without the Use of Amplification," *IEEE Sens. Lett.*, vol. 3, no. 3, 5000204, Mar. 2019.

[103] Y. Sun *et al.*, "Review of a Specialty Fiber for Distributed Acoustic Sensing Technology." *Photonics*, vol. 9, no. 5, 277, Apr. 2022.

[104] C. Wang *et al.*, "Distributed acoustic sensor using broadband weak FBG array for large temperature tolerance." *IEEE Sens. J.*, vol. 18, pp. 2796–2800, Apr. 2018.

[105] D.P. Pallarés-Aldeiturriaga *et al.*, "Optical Fiber Sensors by Direct Laser Processing: A Review," *Sensors*, vol. 20, no. 23, 6971, Dec. 2020.

[106] A. Donko *et al*., "Low-loss micro-machined fiber with Rayleigh backscattering enhanced by two orders of magnitude." In *Proc. Conf. Opt. Fib. Sens.* (p. WF75), Sep 2018.

[107] M. Wu *et al*., "Quasi-distributed fiber-optic acoustic sensing system based on pulse compression technique and phase-noise compensation," *Opt. Lett*., vol. 44, no. 24, pp. 5969 -5972, Dec. 2019.

[108] M. Wu *et al*., "Large-scale multiplexed weak reflector array fabricated with a femtosecond laser for a fiber-optic quasi-distributed acoustic sensing system," *Opt. Lett.*, vol. 45, no. 13, pp. 3685 -3688, Jun. 2020.

[109] B. Redding *et al.*, "Low-noise distributed acoustic sensing using enhanced backscattering fiber with ultra-low-loss point reflectors." *Opt. Express*, vol. 28, no. 10, pp. 14638-14647, Apr. 2020.

[110] D.R. Kharasov *et al.*, "The Maximum Operating Range of a Distributed Sensor Based on a Phase-Sensitive Optical Time-Domain Reflectometer Utilizing Telecommunication Fiber with Reflective Centers." *Moscow Univ. Phys.*, vol. 76, pp. 167–175, May 2021.

[111] D.R. Kharasov *et al.*, "Extending the operation range of a phase-sensitive optical time-domain reflectometer by using fibre with chirped Bragg gratings," *Quantum Electron*, vol. 50, no 5, pp. 510-513, May 2020.

[112] H.M. Ogden *et al.*, "Enhanced bandwidth distributed acoustic sensing using a frequency multiplexed pulse train and micro-machined point reflector fiber," *Opt. Lett.*, vol. 47, no.3, pp. 529-32, Feb. 2022.

[113] L. Zhang *et al*., "Distributed and dynamic strain sensing with high spatial resolution and large measurable strain range" *Opt. Lett.*, vol. 45, no. 18, pp. 5020-5023, Sep 2020.

[114] J. Xiong *et al.,* "Single-Shot COTDR Using Sub-Chirped-Pulse Extraction Algorithm for Distributed Strain Sensing," *J. Lightwave Technol.*, vol. 38, no. 7, pp. 2028-2036, Apr. 2020.

[115] J. Xiong, *et al.* "High sensitivity and large measurable range distributed acoustic sensing with Rayleigh-enhanced fiber," *Opt. Lett.*, vol. 46, no. 11, pp. 2569-2572, May 2021.

[116] A. Masoudi *et al.,* "A 10 cm spatial resolution distributed acoustic sensor based on ultra low-loss enhanced backscattering fibre." *Opt. Continuum*, vol. 1, no.9, Sep. 2022.

[117] A. Masoudi, M. Beresna, G. Brambilla, "152 km-range single-ended distributed acoustic sensor based on inline optical amplification and a micromachined enhanced-backscattering fiber." *Opt. Lett.*, vol. 46, no. 3, pp.552-555, Jan. 2021

[118] L.D. van Putten *et al.*, "Numerical Modelling of a Distributed Acoustic Sensor Based on Ultra-Low Loss-Enhanced Backscattering Fibers," *Sensors*, vol. 21, no. 20, 6869, Oct. 2021.

[119] Y. Deng *et al*., "Quasi-distributed fiber-optic acoustic sensor based on a low coherence light source," *Opt. Lett.*, vol. 47, no. 15, pp. 3780-3782, Jul. 2022.

[120] T. Liu *et al.*, "Ultra-high resolution strain sensor network assisted with an LS-SVM based hysteresis model." *Opto-Electron. Adv*., vol. 4, no. 5, 200037, May 2021.

[121] J. Jiang *et al.*, "Quasi-Distributed Fiber-Optic Acoustic Sensing With MIMO Technology," in *IEEE Internet of Things J.*, vol. 8, no. 20, pp. 15284-15291, Oct. 2021.

[122] Q. Wang *et al*., "Improving OFDR Distributed Fiber Sensing by Fibers With Enhanced Rayleigh Backscattering and Image Processing." *IEEE Sensors J.*, vol. 22, no. 19, pp. 18471-8, Aug. 2022.

[123] S. Kreger *et al.*, "Enhanced Sensitivity High Spatial Resolution Distributed Acoustic Sensing Using Optical Frequency Domain Reflectometry and a Point Reflector Array Sensor," In Proc. of *Optical Fiber Sensors* (pp. T3-75), Jun 2020

[124] V.A. Yatseev, A.M. Zotov and O.V. Butov, "Combined frequency and phase domain time-gated reflectometry based on a fiber with reflection points for absolute measurements," *Res. Phys.*, vol. 19, 103485, Dec. 2020.

[125] H. Li *et al*., "Ultra-High Sensitive Quasi-Distributed Acoustic Sensor Based on Coherent OTDR and Cylindrical Transducer" *J. Lightwave Technol.*, vol. 38, no. 4, pp. 929-938, Feb. 2020.

[126] Q. Liu, *et al.*, "High resolution and large sensing range liquid level measurement using phase-sensitive optic distributed sensor," *Opt. Express*, vol. 29, no. 8, pp. 11538-11547, Mar. 2021.

[127] R.A. Perez-Herrera *et al.*, Optical fiber lasers assisted by microdrilled optical fiber tapers," *Opt. Lett.*, vol. 44, no. 11, pp. 2669–2672, May 2019.

[128] S.M. Popov *et al.*, "Optical fibres with an inscribed fibre Bragg grating array for sensor systems and random lasers." *Quantum Electron*., vol. 51, no. 12, pp. 1101-1106, Dec. 2021.

[129] X. Lu *et al*., "Impact of fiber coating on the temperature response of distributed optical fiber sensors at cryogenic ranges*", J. Lightwave Technol.*, vol. 36, no. 4, pp. 961-967

[130] R.R. Preizier *et al.*, "On the actual bandwidth of some dynamic fiber optic strain/temperature interrogators" *SPIE Proc.,* vol 10323, art. 103235C, 2017.

[131] C X. Tan *et al*., "Strain transfer effect in distributed fiber optic sensors under an arbitrary field." *Autom. Constr.*, vol. 124 , art. no. 103597, 2021
[132] M. Tan *et al*., "Strain transfer effect on measurements with distributed fiber optic sensors." *Autom. Constr.*, vol. 139, at. 104262, 2022
[133] S. Mahjoubi *et al.*, "Inverse analysis of strain distribution sensed by distributed fiber optic sensors subject to strain transfer." *Mech. Syste. Signal. Proc.,* Vol. 166, art. 108474, 2022
[134] X. Chapelau, and A. Bassil "A general solution to determine strain profile in the core of distributed fiber optic sensors under any arbitrary strain fields" *Sensors*, Vol. 21, no. 16, pp. 5423, Aug. 2021
[135] Y. Yao *et al.* " Measurement of cable forces for automated monitoring of engineering structures using fiber optic sensors: A review." *Autom. Constr.*, vol. 126, no. 103687, June 2021.

Timothy Lee obtained his PhD in 2013 at the University of Southampton's Optoelectronics Research Centre, where he now works as a Senior Research Fellow. His research focuses on ultrafast laser material processing, in particular direct writing of fiber and photonic devices such as waveguides and gratings, with diverse applications ranging from optical fiber sensing and metrology to telecommunications. Other research interests include microfibers, nonlinear optics and optical resonators. He has published over 100 peer-reviewed papers in journals and conferences, co-authored a book chapter, and served on the committee for the Photonics West conference LAMOM. Dr Lee also holds a MEng degree (1st class honors) in Electronic Engineering from the University of Southampton.

Martynas Beresna received B.S. degree in Physics from Vilnius University, Lithuania in 2008 and his PhD in Optoelectronics in 2012 from University of Southampton, UK. His research interests cover optical fiber sensors and laser material processing. In 2016 he was awarded the RAEng research fellowships for his work on fs laser structuring of glass. Since 2022 he has been Principal Research Fellow at the Optoelectronics Research Centre.

Ali Masoudi is a Senior Research Fellow at the Optoelectronics Research Centre (ORC), University of Southampton, and leads the distributed optical fiber sensing group at the ORC. He received his PhD degree in 2014 for his work on distributed acoustic sensors. After receiving his PhD, Dr Masoudi designed and developed portable DAS units which he subsequently used in several industrial collaborations with entities such as Network Rail, BT, and Carbon trust. The DAS unit has also been used in several interdisciplinary collaborations with other research institutes such as Network Rail, the Institute of Sound and Vibration Research (ISVR), and National Oceanography Centre (NOC). He has authored 3 patents and published more than 60 papers in scientific journals and international conferences and has presented his research as an invited and keynote speaker on 7 different occasions.

Gilberto Brambilla obtained his degree in Engineering (materials) with honors at Politecnico di Milano (Milan, Italy) in 1996 and his PhD in Optoelectronics in 2002 at the Optoelectronics Research Centre (ORC), within the University of Southampton (United Kingdom). His research includes optical fiber sensors, specialty optical fibers, fiber devices, manufacturing and lasers.

He is currently Deputy Director and General Manager of The Future Photonics Hub and Professor in Photonics at the ORC, where he leads the group of Optical Fiber Sensors and Devices. He has been Director of the Centre for Innovative Manufacturing in Photonics until 2015. He was awarded the Royal Society University Fellowship in 2007, which was then renewed. He has published more than 350 papers in academic journals and conference proceedings, he authored 10 patents, and he has given more than 40 plenary/keynote/invited talks or tutorials at international conferences.

Prof. Brambilla is a member of IEEE and of IEEE Photonics conference council. He is Deputy Editor of Optical Fiber Technology and has been associate editor of IEEE Photonics Technology Letter for a decade, until 2022.